Available online at www.sciencedirect.com
SCIENCE DIRECT®
Polymer 44 (2003) 8155–8165
polymer
www.elsevier.com/locate/polymer

# Surface morphology control of immiscible polymer-blend thin films

Xue Li, Yanchun Han*, Lijia An*

*State Key Laboratory of Polymer Physics and Chemistry, Changchun Institute of Applied Chemistry, Chinese Academy of Sciences, No 5625 Renmin Street, Changchun 130022, People's Republic of China*

Received 25 May 2003; received in revised form 15 August 2003; accepted 8 October 2003

**Abstract**

The effects of the molecular weights (molecular weight of polystyrene, $M_{w,PS}$, varying from 2.9 to 129 k) on the surface morphologies of spin-coated and annealed polystyrene/poly (methyl methacrylate) (PS/PMMA = 50/50, w/w) blend films were investigated by atomic force microscopy and X-ray photoelectron spectroscopy. For the spin-coated films, when the $M_{w,PS}$ varied from 2.9 to 129 k, three different kinds of surface morphologies (a nanophase-separated morphology, a PMMA cellular or network-like morphology whose meshes filled with PS, a sea-island like morphology) were observed and their formation mechanisms are discussed, respectively. Upon annealing, two different morphology-evolution processes were observed. It is found that a upper PS-rich phase layer is formed when $M_{w,PS} < 4$ k, and this behavior is mainly attributed to the low interfacial tension between PS and PMMA component. When $M_{w,PS} > 4$ k, the PS-rich phase forms droplets on top of the PMMA-rich phase layer which wets the $SiO_x$ substrate. These results indicate that the surface morphology of the polymer blend films can be controlled by the polymer molecular weight and annealing conditions.


*Keywords:* Polystyrene; Poly (methyl methacrylate); Atomic force microscopy

## 1. Introduction

Strongly incompatible polymers, such as polystyrene/-poly (methyl methacrylate) (PS/PMMA), polystyrene/poly (vinyl pyridine) (PS/PVP), have been studied intensively because these polymer pairs are involved in many potential practical applications [1–3]. These technological interests motivate many fundamental studies of morphological control of phase separating polymer mixtures. To particular requirements, such as surface coatings, how to create and control films with different properties is very important. It has been shown that the phase morphology depends on polymer molecular structures, composition, molecular weights, and the method of blend preparation [4] and can also be influenced by a suitable choice of the substrate surface free energy [1]. The effects of molecular weights on surface morphology and surface enrichment focused on partially compatible polymer blends have been studied theoretically [5–7] and experimentally [8–12]. For incompatible polymer blends, although many studies on the surface morphology formation had been reported [13–15], a systematic study of the surface morphologies of spin-cast polymer blend films as a function of molecular weight of components hasn't been made. Geoghegan et al. [16] reported the effects of molecular weight on the morphology in as cast PS/polybutadiene (PB) blend films. The results show that the surface enrichment is dependent on molecular weight and stratified films can be created by changing the molecular weight of the components [13]. For a blend of high-$M_w$ PS and low-$M_w$ PMMA, anomalous behavior was observed. Low-PMMA preferentially segregated at the air–polymer interface though it had a higher surface energy [17]. The results of Hariharan [7] also showed that the surface might be favorably covered by the low $M_n$ component because a longer polymer chain at the surface suffered a severe conformational entropic penalty [18].

The surface structures of the incompatible polymer blend films obtained by means of spin-coating are not in thermodynamic equilibrium state [15,19–24]. To reduce the interfacial tension, the coarsening of the domains near to the surface to equilibrium will take place upon annealing. For PS/PMMA systems, the molecular weights used in previous investigations are between 20 and 100 k [15,21–24]. In this molecular weight range, the difference

* Corresponding author. Tel.: +86-431-5262175; fax: +86-431-5262122.
*E-mail addresses:* ychan@ns.ciac.jl.cn (Y. Han), ljan@ns.ciac.jl.cn (L. An).

0032-3861/$ - see front matter © 2003 Elsevier Ltd. All rights reserved.
doi:10.1016/j.polymer.2003.10.012

in molecular weight is not sufficiently affecting the surface and interfacial energies. Hence, Harris et al. [24] conclude that PS does not form an overlayer in PS/PMMA blend films with morphologies near thermodynamic equilibrium. The PS forms droplets of a large size range on top of a PMMA layer that wets the hydrophilic $SiO_x$ substrate.

Interfacial tension ($\gamma$) between the components of the blend is one of the parameters that describe the thermodynamics of the blends. When the molecular weight of only one polymer type is varied, the $\gamma$ increases rapidly with molecular weight and reach a plateau value at a molecular weight [25]. Fig. 1 shows the schematic representation of the molecular weight dependence of interfacial tension for binary polymer blend. In region I, $\gamma$ decreases greatly with the decrease of $M_w$. The low $\gamma$ value is expected to influence the surface morphology of a blend film. Till now, few papers [17] regarding the effect of molecular weight, especially in the low molecular weight range ($\gamma$ is in the region I as shown in Fig. 1), on the surface structure of the blend film are reported.

In this work, the influences of the molecular weight of PS on the morphologies of the spin-coated and the annealed PS/PMMA blend films were investigated. The molecular weights have an important effect on the surface morphology of a spin-coated film. Upon annealing, we found that a PS-rich phase surface layer is formed when the molecular weight of PS is lower than the particular value (about 4 k in this work). This result is in contrast to the recent results [15,24]. When the molecular weight of PS is higher than 4 k, the PS-rich phase forms droplets on top of the PMMA-rich phase layer which is consistent with the reference results [15,24].

## 2. Experimental

### 2.1. Material

Polystyrene standard (PS-6 and PS-8) and poly (methyl methacrylate) (PMMA) were purchased from Aldrich Chemical Company and used as received. The others of polystyrene standard were obtained from Nanjing University, P. R. China. Their characteristics are shown in Table 1. The molecular weight $M_w$ and polydispersity $M_w/M_n$ were determined by GPC. The glass transition temperature was measured by DSC. The solvent toluene for spin-coating was analytical grade.

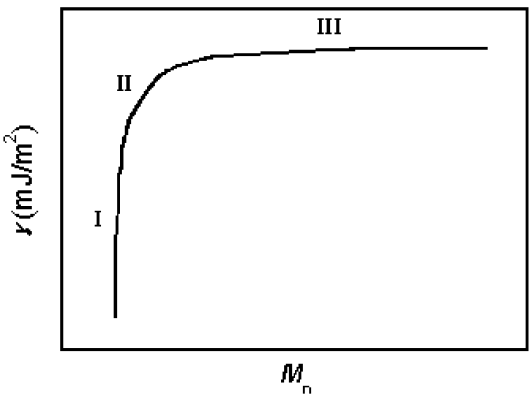


Fig. 1. The schematic representation of the molecular weight dependence of interfacial tension for binary polymer blend.

### 2.2. Film preparation

The polymer solutions were prepared by dissolving a mixture of 50% PS and 50% PMMA (w/w) in toluene. Prior to spin coating, the polymer solutions were filtered with 0.22 μm Millipore membrane. The silicon wafers were cleaned with a mixed solution of concentrated $H_2SO_4$ and $H_2O_2$ (30%) (70/30 v/v) at 110 °C for 1 h, then the wafers were rinsed in deionized water for several times and dried.

The blend films were prepared from PS/PMMA solutions (typically 1.0 wt% polymer) with a KW-4A Precision Spin-Coater (Chemat Technology, Inc.) in a glove box. The spin-coating was carried out at 2000 rpm at room temperature. All the spin-coated films were dried in a vacuum for 10 h at 50 °C. The thicknesses of the PS/PMMA blend films ranged from 70 to 90 nm.

### 2.3. Atomic force microscopy

The atomic force microscopy (AFM) measurements of the blend films were performed on SPA300HV with SPI3800 controller, Seiko Instruments Industry, Co., Ltd. Images of the surface morphologies of the films were made with AFM in the contact mode and friction force microscopy (FFM) images was also performed simultaneously with topographical imaging. Some samples were measured with dynamic mode atomic force microscopy (DFM). The cantilever driving amplitude $A_0$ was fixed and the images were recorded at a high set point value (light tapping). The cantilever used in this work was fabricated from $Si_3N_4$. The tip types in the AFM and the DFM measurements were SN-AF01 and SI-DF3, respectively. The spring constant and the resonance frequency of SI-DF3 were 1.9 N/m and 28 kHz, respectively.

Table 1
Characteristics of PS and PMMA

| Polymer | $M_w$ ($\times 10^4$) | $M_n$ ($\times 10^4$) | $M_w/M_n$ | $T_g$ (°C) | $\eta_0$ (Pa s) |
|---|---|---|---|---|---|
| PMMA | 10.26 | 4.83 | 2.12 | 109 | $3.3 \times 10^7$ |
| PS-1 | 0.29 | 0.28 | 1.05 | 62 | – |
| PS-2 | 0.40 | 0.39 | 1.03 | 62 | – |
| PS-3 | 0.56 | 0.55 | 1.02 | 84 | $4.4 \times 10^2$ |
| PS-4 | 0.71 | 0.69 | 1.03 | 87 | $8.0 \times 10^2$ |
| PS-5 | 1.00 | 0.96 | 1.06 | 85 | $1.9 \times 10^3$ |
| PS-6 | 3.16 | 2.91 | 1.08 | 103 | $2.0 \times 10^4$ |
| PS-7 | 6.50 | 6.13 | 1.06 | 107 | $1.8 \times 10^5$ |
| PS-8 | 12.90 | 12.10 | 1.06 | 107 | $2.1 \times 10^6$ |

### 2.4. X-ray photoelectron spectroscopy

The X-ray photoelectron spectroscopy (XPS) was measured with VG ESCALAB MK at room temperature by using an Mg $K_\alpha$ X-ray source ($h\nu = 1253.6$ eV) at 14 kV and 20 mA. The sample analysis chamber of the XPS instrument was maintained at a pressure of $1 \times 10^{-7}$ Pa. X-ray beam was perpendicular incidence to the sample surface in all measurements and the maximum sampling depths was less than 10 nm. All the C1s peaks were calibrated to the standard binding energy of 284.6 eV for neutral carbon in order to correct the charging energy shifts. A linear-background method removed the XPS background and the peaks analysis carried out by using the curve-fitting software.

## 3. Results and discussion

### 3.1. Effects of molecular weight on the surface morphologies of spin-coated films

When the $M_{w,PS}$ varied from 2.9 to 129 k, three kinds of surface morphologies were observed: a nanophase-separated morphology, a PMMA cellular or network-like morphology whose meshes filled with PS, a sea-island like morphology (Fig. 2).

When $M_{w,PS} \leq 4$ k, nano-phase separation is dominant in surface morphology formation. Fig. 2a reveals that the phase-separated morphology is not distinct and the domain size at the film surface is very small (ca 100 nm) when $M_{w,PS} \leq 4$ k. The AFM image of the sample treated with cyclohexane for 3 min (PS is etched and PMMA is not etched by cyclohexane) [15,24] also verifies the average lateral structures is less 100 nm (Fig. 2b). DFM observation [26–32] illustrated that the bright parts correspond to PS matrix and the black parts to PMMA domains (Fig. 3). It showed that only small amount of the island-like surface domains in Fig. 2a is composed of PMMA-rich phase and most of them are composed of PS-rich phase. When $M_{w,PS} = 4$ k, small pits (100–150 nm) appears in Fig. 2d suggesting that the phase domains begin to largen.

As $M_{w,PS}$ was ranged between 5.6 and 31.6 k, a cellular or network-like surface morphology of the PS/PMMA blend film was observed (Fig. 2e, g, i and k). After the sample was treated with cyclohexane, similar morphologies were observed (Fig. 2f, h, j and l) only with the increase of topographic variation. Therefore, the PMMA-rich phases form the network and the meshes are filled by the PS-rich phases. As the $M_{w,PS}$ increased to 31.6 k, the surface has the topographic feature as if the nets of Fig. 2i are filled in by PS (Fig. 2l).

As the $M_{w,PS}$ is increased to 65 k, one can see from Fig. 2m and n that the islands formed by PMMA-rich phase (bright parts) appear at the surface, the PS-rich phases form the matrix (dark parts). As the $M_{w,PS}$ is increased further, the surface morphologies of the PS/PMMA blend films all show the similar phase-separated structures (Fig. 2o and p), that is, the protruded PMMA islands disperse in the PS-rich matrix [15].

The change in molecular weight will cause a difference in the miscibility of PS/PMMA blends and a difference in the relative viscosity of two polymers in solution. It is well known that the zero-shear viscosity ($\eta_0$) of the flexible linear polymers has established two regions, which are separated by a characteristic molecular weight $M_{w,c}$. In melt or concentrated solution, low molecular weight PS moves independently, but the movements of high molecular weight PS are retarded by entanglements. During the late stage of spin-coating, owing to the evaporation of solvent, the viscosity or the molecular weight of the sample will play an important role.

Although the viscosity of PS component is very low when the $M_{w,PS} \leq 4$ k, the miscibility between PS and PMMA will play a dominant role in determining the initial morphology after spin-coating. Once the phase separation took place during spin coating, the PMMA-rich phase was more quickly depleted of the solvent and solidified on the hydrophilic substrate and could aggregate to form PMMA-rich phase layer, and PS liquid phase might form the upper layer. Generally, the upper PS layer on PMMA is unstable and will dewet as more solvent evaporated [15,34]. However, for low molecular weight polymers, the combinatorial entropy of mixing becomes large and the miscibility between PS and PMMA tends to increase as the PS molecular weight decrease [35,36]. This means that a fraction of low molecular weight PS component will reside at the PMMA-rich phase, and the interfacial tension will be lowered. Therefore, the coarsening or dewetting process of PS-rich phase layer at late stage of spin-coating may slow down. Further evaporation of the solvent left the nanosize domains at the film surface (Fig. 4c). The phenomenon may be of great importance in many applications. For example, it has been illustrated that the nanophase-separated polymer films may be used as antireflection coatings [2].

When the $M_{w,PS}$ is between 5.6 and 31.6 k, which is less than the characteristic molecular weight (35 k) of PS, the viscosity of the PS component will play an important role in the structure formation. During the spin-coating process, the depleted PMMA-rich phase first formed the small particles; the small PMMA particles collide via Brownian motion and adhere to each other to form aggregates. Owing to the viscosity of PS component was small, the larger aggregates can also move by local surface flow and form network-like structures very quickly (the driving force is the attractive interactions between aggregates). This may be similar to the first stage of phase separation of the colloidal suspensions system [33], in which a particle network formed initially. When the solvent evaporates further during the spin-coating, the network-like PMMA domains in Fig. 2e–i are frozen at the surface of the film. At this point, the PS-rich phase is still swollen and dispersed over the meshes. At late

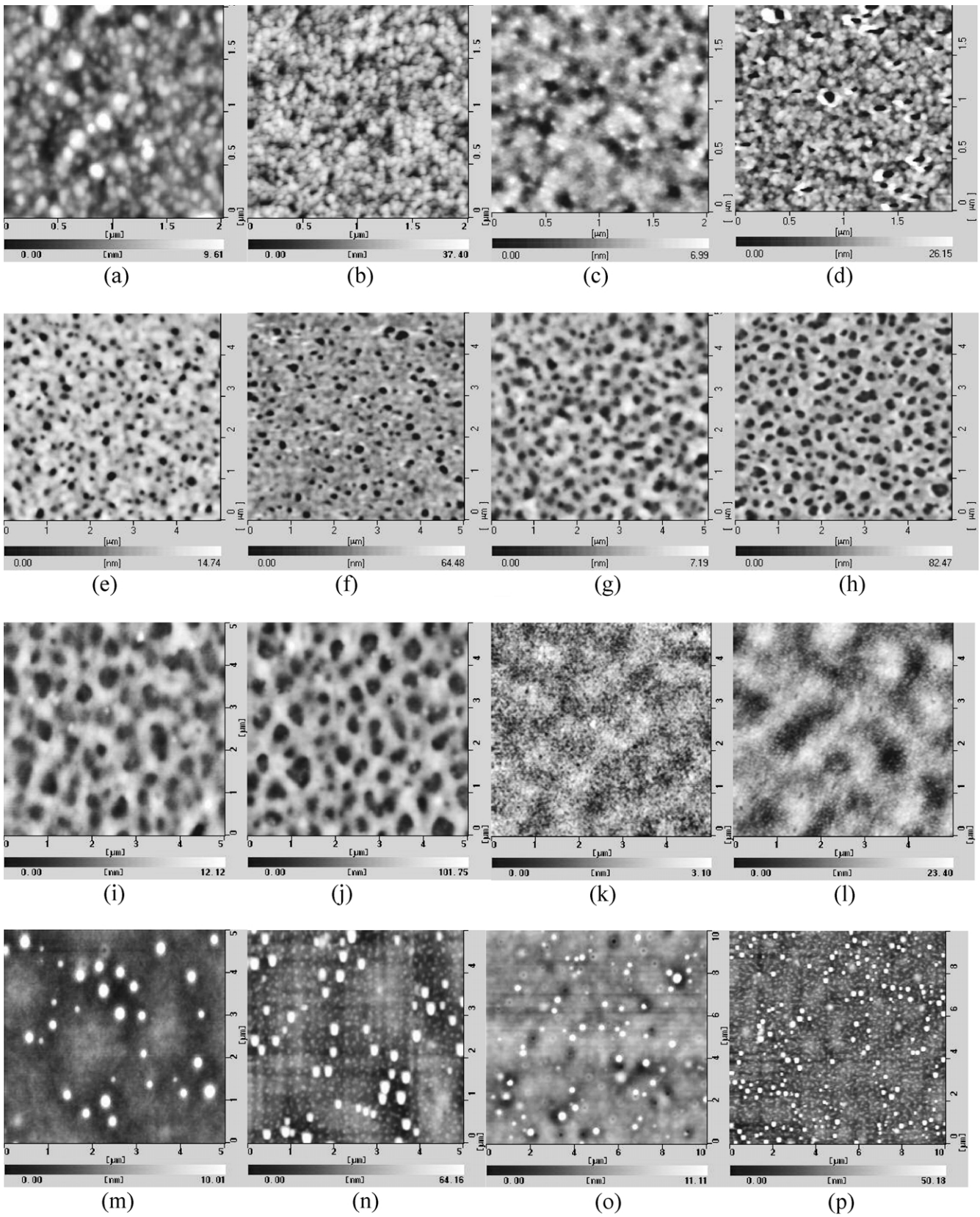


Fig. 2. AFM topography of thin PS/PMMA blend films with different PS molecular weights. ((a), (c), (e), (g), (i), (k), (m), (o): as spin-coated. (b), (d), (f), (h), (j), (l), (n), (p): All the samples were etched with cyclohexane for 3 min). $M_{w,PS}$: (a), (b) 2.9 k; (c), (d) 4.0 k; (e), (f) 5.6 k; (g), (h) 7.1 k; (i), (j) 10 k; (k), (l) 31.6 k; (m), (n) 65 k; (o), (p) 129 k.

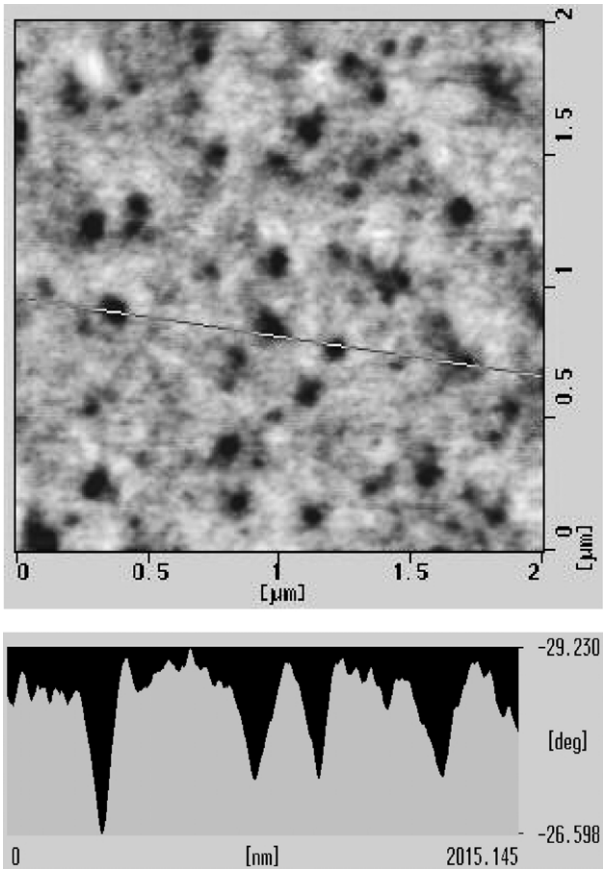


Fig. 3. DFM phase image and its sectional views along the lines in the images for the spin-coated PS-1/PMMA blend film.

stage, the PS-rich phase collapsed to form network-like structure (Fig. 4d).

When the $M_{w,PS}$ is increased further, as reported in Refs. [13–15], the surface morphologies in Fig. 2m and o can be explained as follows when the molecular weight of PS is greater than the characteristic molecular weight $M_{w,c}$ of PS (35 k). Toluene is a better solvent for PS than for PMMA. The PS-rich phase has higher toluene content than the PMMA-rich phase during spin-coating. The solvent evaporates faster from the PMMA-rich phase, which is more quickly depleted of the solvent and solidifies first onto the substrate and leads to more PMMA-rich phases near the substrate. Owing to the viscosity of the PS component is great at late stage of spin-coating, the further coarsening of the PMMA-rich phase could not go along. In turn, the PS-rich phase is still swollen. As the solvent evaporates finally from the PS phase, it collapses and form lower regions of the free surface (Fig. 4e).

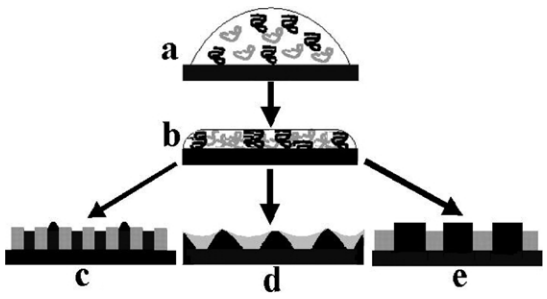


Fig. 4. Schematic drawings show the effect of the molecular weight, $M_{w,PS}$, on the formation of the surface phase-separated structure of the PS/PMMA blend film during spin-coating process. The homogeneous PS and PMMA mixture solution is deposited on the substrate (a). During spin-coating process, the solution film thins, the solvent evaporates and the PMMA-rich phase (black) and the PS-rich phase (white) begin to form (b). When the $M_{w,PS} < 4$ k, mainly due to the increase of the miscibility between PS and PMMA, nanophase separation is dominant (c). With the increase of $M_{w,PS}$ (which is higher than 4 k but less than 35 k), owing to the low viscosity of PS component, PMMA-rich phases form network-like structure whose meshes filled with PS (d). When the $M_{w,PS}$ is increased further, a completed phase-separated structure with elevated PMMA islands is formed (e).

### 3.2. *Effects of molecular weight on the thermal stability of the blend films*

Recently, Harris et al. [24] studied the surface morphologies of annealed PS/PMMA ($M_{w,PS} = 20,870, M_{w,PMMA} \geq 21,530$) thin films on silicon substrates. The results show that the PS always forms droplets of a large size range on top of a PMMA layer that wets the $SiO_x$ substrate and dose not form an overlayer in samples with morphologies near thermodynamic equilibrium. However, when PS/PMMA films with different PS molecular weights were annealed at 156 °C for various times, a distinct difference in the surface morphologies of the PS/PMMA blend films was observed when $M_{w,PS}$ was changed from $M_{w,PS}$ below 4 k to $M_{w,PS}$ above 4 k.

To further understand the morphology changes of the PS/PMMA blend films, Fig. 5 shows the surface morphologies of PS-1/PMMA blend films after annealed for different times. To identify whether the bright parts in the AFM images were corresponding to PMMA- or PS-rich phases, the friction images and their line profile were also taken (Fig. 5a′–c′). The bright parts and dark parts in the friction images are corresponding to the PMMA- and the PS-rich phases, respectively [37]. On annealing for 40 min, the PMMA-rich phase depressed and formed the pits at the surface (Fig. 5a). When the film was annealed for 82 h, FFM image displays similar contrast (Fig. 5c′). This indicates that the whole surface of the annealed film is covered by a single PS-rich phase. When the film was annealed for 8 days, a striking result is that the PS-1/PMMA blend film is still stable and its surface is very smooth. XPS measurements were performed to evaluate the surface composition. Fig. 6a shows the XPS C1s spectrum with fitted curve (Fig. 6b) for the annealed PS-1/PMMA blend film. The C1s peaks at 286.1 and 288.4 eV, which are assigned to ether carbon and carbonyl carbon, were not observed. However, the C1s shake-up peak corresponding to $\pi-\pi^*$ transition of the benzene ring is obvious. This also indicates that PS has segregated to the free surface and formed a upper PS-rich phase layer. After the sample was treated with cyclohexane for 3 min, the XPS C1s spectrum shown in Fig. 6c is completely corresponding to the C1s of pure PMMA and no

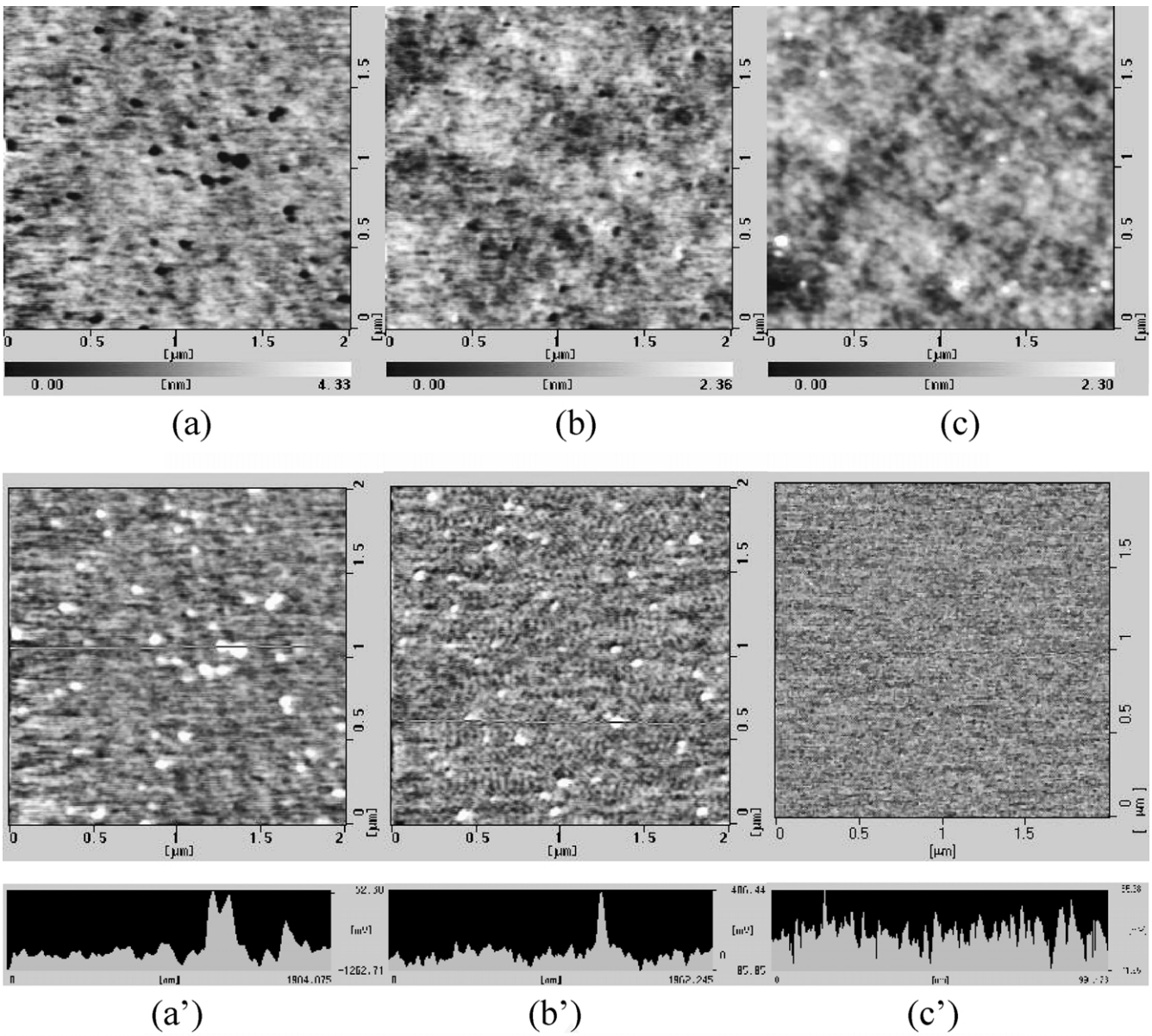


Fig. 5. AFM topographical (up) and frictional (down) images of PS-1/PMMA blend films showing changes in surface structure upon annealing at 156 °C. Annealing times: (a) 40 min; (b) 6 h; (c) 82 h.

silicon was detected (Fig. 6d). This indicates that the substrate is covered by PMMA-rich phase. To investigate the film structure further, a scratch was made in the film and the AFM images and their cross-sectional views before and after etching with cyclohexane are displayed in Fig. 7a–c, respectively. After etching, the PMMA-rich phase has become network-like morphology. The surface is rough and the bottom of a mesh is also covered by PMMA-rich phase domains (Fig. 7c). Compared the height variation between Fig. 7a and b, one can conclude that the film surface is covered completely by PS. Combining the results of Figs. 6 and 7, a schematic illustration of the annealed film morphology is shown in Fig. 7c.

The important factor affecting the film stabilization is the interface between PS and PMAM. It has been reported theoretically that interfacial tension between two polymers depends on the molecular weight and could be expressed as [38]

$$\gamma = \gamma_\infty\left(1 - \frac{\pi^2}{12\chi}\left(\frac{1}{N_1} + \frac{1}{N_2}\right)\right) \tag{1}$$

and the interfacial width is

$$w = \frac{2a}{\sqrt{6\chi}}\left(1 + \frac{\ln 2}{\chi}\left(\frac{1}{N_1} + \frac{1}{N_2}\right)\right) \tag{2}$$

where $\gamma_\infty$ is the value of the interfacial tension for the approximation of infinite $M_w$. $\chi$ and $a$ are the Flory–Huggins interaction parameter and the polymer statistical segment length (the Kuhn segment length). $N_1$ and $N_2$ are the degree of polymerization of the two polymers.

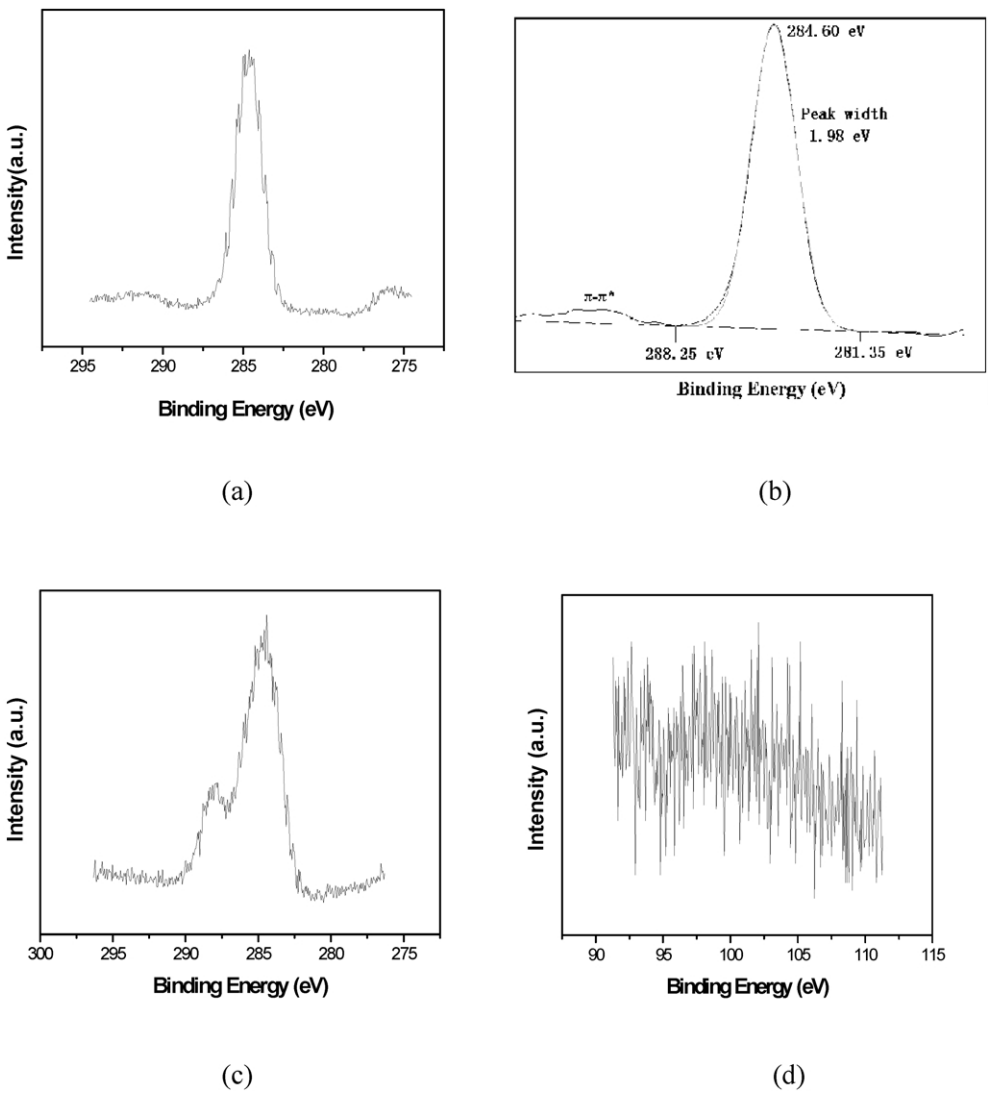


Fig. 6. XPS C1s spectrum (a) with fitted curve (b) for the PS-1/PMMA film after annealing at 156 °C for 8 days. After the sample (a) was etched with cyclohexane for 3 min, the XPS C1s and Si spectra are shown in (c) and (d), respectively.

Using the Eqs. (1) and (2), the interfacial tension and the interfacial width can be calculated. Because the Kuhn segment length is an experimentally extremely difficult to handle quantity even if it is well defined within the concept of random walk statistics, thus an average of the two polymers must be used [39]. For the system PS/PMMA, Higashida et al. [40] used $a = 0.8$ nm and Sferrazza et al. [36] took $a = 0.7$ nm. For the parameter $\chi$, the measured values are wide scattering though $\chi$ values of PS and PMMA are known for various temperatures. $\chi = 0.037$ was took by Sferrazza et al. [36] to calculate the interfacial width for PS/PMMA blend. $\chi$ determined from ellipsometric measurements was 0.0529 at 150 °C and 0.0262 at 160 °C, respectively, [40]. For our temperature the value $\chi = 0.037$ was taken. Using the Eqs. (1) and (2), with $a = 0.7$ nm, and $\gamma_\infty = 1.7$ mJ/m$^2$ [36], the interfacial tension and the interfacial width were calculated and listed in Table 2. It can be seen that the interfacial tension of PS/PMMA is reduced greatly when the $M_{w,PS} < 4$ k. It seems that the stabilization of the top PS-rich phase layer is mainly caused by the decrease of the interfacial tension between PS and PMMA. Apart from this reason, the surface tension of PS

Table 2
The interfacial tension and interfacial width between PS and PMMA calculated by Eqs. (1) and (2)

| | PS-1/PMMA | PS-2/PMMA | PS-3/PMMA | PS-4/PMMA | PS-5/PMMA | PS-6/PMMA | PS-7/PMMA | PS-8/PMMA |
|---|---|---|---|---|---|---|---|---|
| $\gamma$ (mJ/m$^2$) | 0.2 | 0.6 | 0.9 | 1.1 | 1.2 | 1.5 | 1.6 | 1.6 |
| $w$ (nm) | 5.1 | 4.5 | 4.1 | 3.9 | 3.7 | 3.3 | 3.2 | 3.1 |

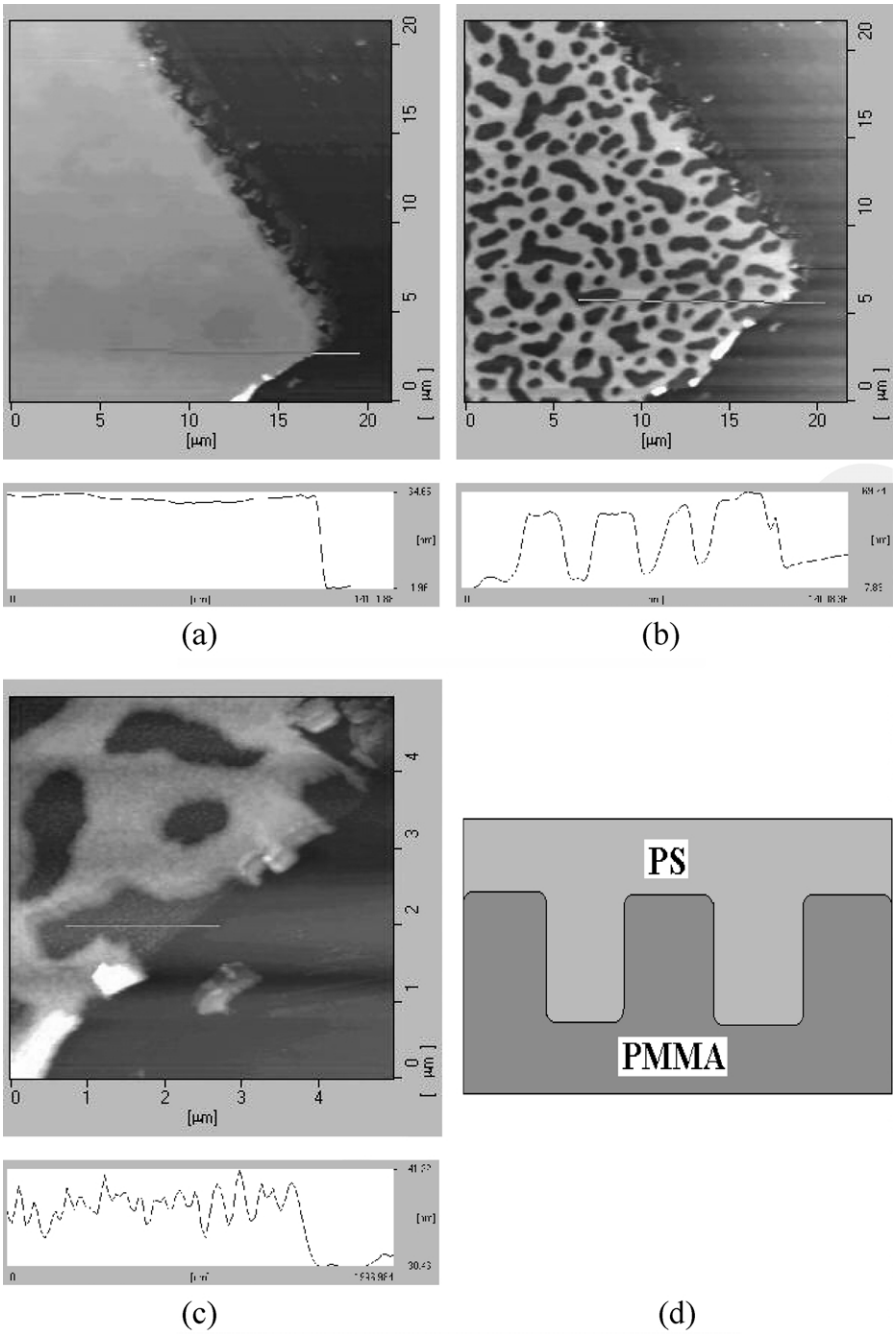


Fig. 7. AFM topographical image and sectional view along the line in the image for the thin PS-1/PMMA blend film, which had been annealed at 156 °C for 8 days. (a) Before etching; (b) and (c) after etching with cyclohexane for 3 min, (c) only at a higher spatial resolution. (d) the overall phase morphology.

also decreases for the low molecular weight PS ($\Gamma = \Gamma_\infty - KM_n^{-2/3}$, where $K$ is constant and $\Gamma_\infty$ is surface tension at infinite molecular weight) [41], which is in favor of the PS-rich phase layer formation at polymer–air surface.

When $M_{w,PS} > 4$ k, the changes of the surface morphologies of annealed PS/PMMA blend films shows the similar trend. In the most mobile system investigated here (PS-3, $M_{w,PS} = 5.6$ k), as shown in Fig. 8, the PS-rich phases form droplets very quickly. After long time annealing (8 days), the same type of droplet morphology as in Ref. [24] is found.

At a higher PS molecular weight, the rate of forming PS droplets will decrease due to the increase of the viscosity. To see the process clearly, Fig. 9 shows the surface morphology changes of a PS-7/PMMA blend film. At beginning of annealing, the PMMA islands depressed and formed pits at the surface. This is mainly caused by the phase separation of PS and PMMA. With the increase of

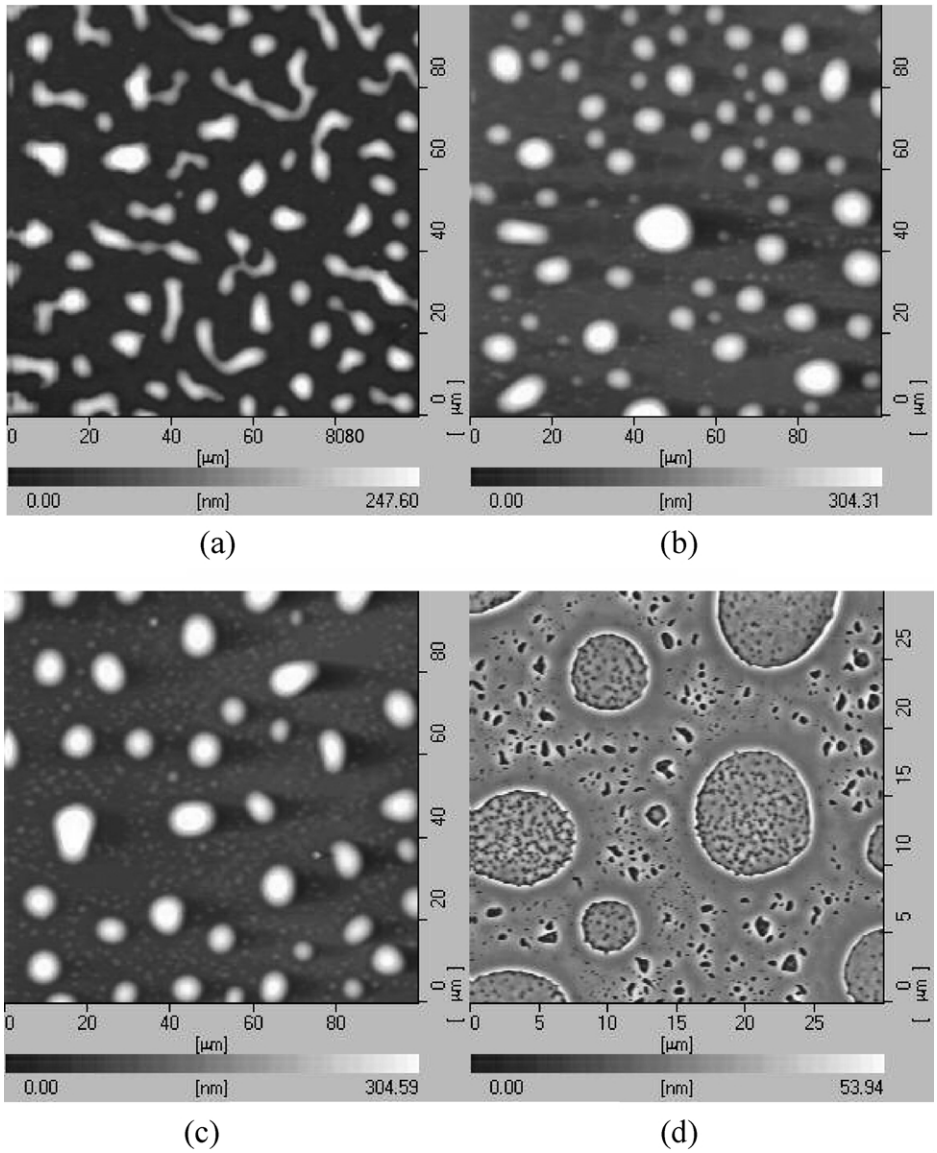


Fig. 8. AFM topographical images of PS-3/PMMA blend films showing changes in surface topography upon annealing at 156 °C. Annealing times: (a) 30 min; (b) 8 h; (c) 8 days. (d) the sample of (c) was etched with cyclohexane for 3 min.

annealing time, similar to the dewetting behavior of a bilayer, where the PS was on the top of the PMMA film, [42] holes on the PS-rich phase layer formed. Then the holes grew up and impinged continuously to form a continuous structure. When annealing further, the continuous PS phase formed separate domains, which could be removed by washing the sample with cyclohexane (Fig. 9e). At last, the spherical PS drops are suspended in a PMMA film [15,24].

Because a variation of the molecular weight is expected to produce different wetting layer thickness in spin-cast polymer blend films [43], the difference in the morphologies observed for PS/PMMA films with different $M_{w,PS}$ lead one to the following question: is the stability change of the blend films caused by a different PS-rich phase layer thickness? To address this question, the zero-shear viscosities $\eta_0$ for PS at 156 °C were calculated by [44,45]

$$\log(\eta_T/\eta_{217}) = 2.68 \times 10^{16}(1/T^6 - 1/\overline{490^6})e^{-1330/M} \quad (3)$$

$$\log \eta_{217} = 3.4 \log \bar{M}_w - 13.40 \qquad (\bar{M}_w \geq 38,000) \quad (4)$$

$$\log \eta_{217} \cong 1.65 \log M - 5.38 \; 38,000 \geq \bar{M}_n \geq 4000 \quad (5)$$

For PMMA, the date ($T_0 = 190$ °C, $C_1 = 9.1$, $C_2 = 195$ and $\eta_{190} = 4.0 \times 10^5$ Pa s) of a commercial sample (Aldrich Chemical Co.) in Ref. [45] was used to estimate the $\eta_0$ of PMMA at 156 °C by

$$\log a_T = -\frac{C_1(T - T_0)}{C_2 + (T - T_0)} \quad (6)$$

The results are also listed in Table 1. The viscosities of PS components used in this work are less than that of PMMA

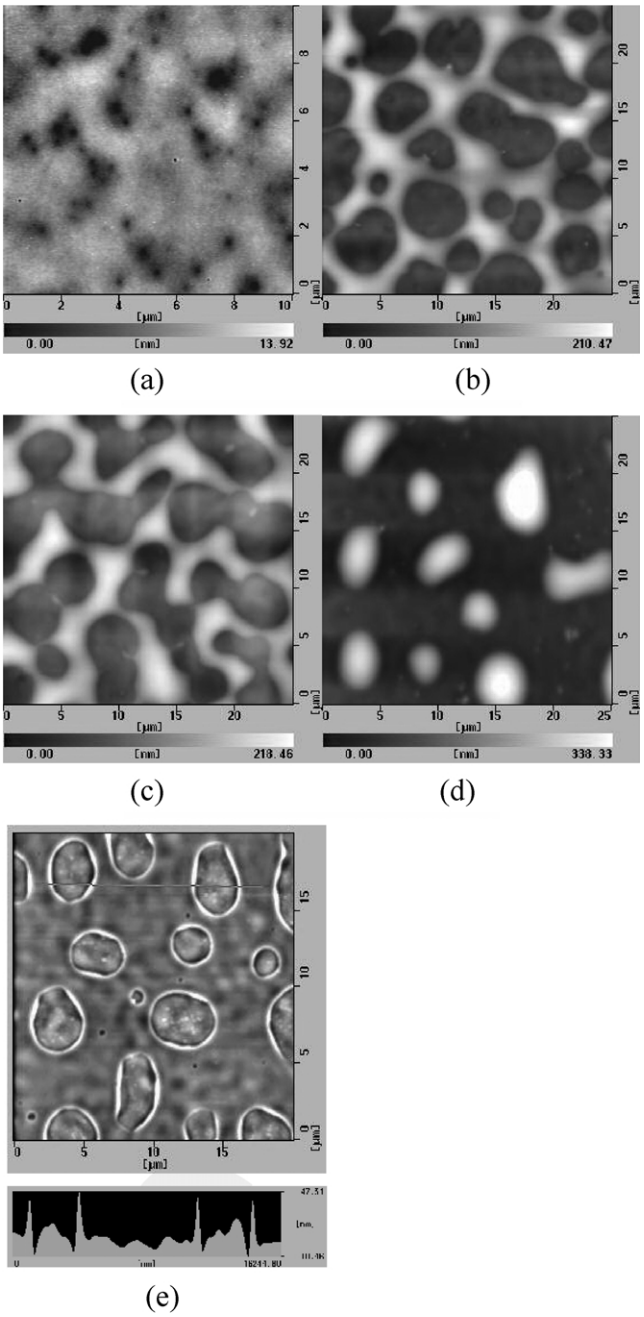


Fig. 9. AFM topographical images of PS-7/PMMA blend films showing changes in surface topography upon annealing at 156 °C. Annealing times: (a) 40 min; (b) 8 h; (c) 14 h; (d) 89 h. (e) showing the AFM topographical image and sectional view along the line in the image of the sample having been annealed for 89 h and etched with cyclohexane for 3 min.

component; the low layer PMMA-rich phase can be considered as solidlike substrate. Therefore, it is deduced that the dewetting speed is independent of the thickness of the PS-rich phase layer [43]. The decrease of evolution velocity is mainly caused by the increase of $M_{w,PS}$.

One can see from the above results that a distinct transition of morphology evolution of the PS/PMMA blend films was observed when $M_{w,PS}$ was varied from 2.9 to 5.6 k. When $M_{w,PS} < 4$ k, the upper PS-rich phase layer is formed due to low interfacial tension between PS and PMMA. When $M_{w,PS} > 4$ k, the PS-rich phase dewet the PMMA-rich phase layer next to the substrate and form PS droplets on top of the PMMA layer that wet the silicon substrate.

## 4. Conclusions

A systematic study of the surface morphologies and thermal stabilities of PS/PMMA blend films as a function of molecular weight of PS ($M_{w,PS}$) was carried out by AFM and XPS. For the spin-coated films, three different kinds of surface morphologies (a nanophase-separated morphology, a PMMA cellular or network-like morphology whose meshes are filled with PS, a sea-island like morphology) were observed when the $M_{w,PS}$ varied from 2.9 to 129 k. The results show that the surface morphology of a polymer blend film can be controlled by varying the molecular weight of one polymer.

Upon annealing, two types of surface morphology evolution processes of the PS/PMMA blend films were observed when $M_{w,PS}$ was varied from 2.9 to 129 k. When $M_{w,PS} < 4$ k, a upper PS-rich phase layer is formed. This structure can greatly suppress the dewetting of PS upper layer on PMMA when annealing at high temperature and may be used to create stable polymer blend films or coatings. Whereas when $M_{w,PS} > 4$ k, the PS-rich phase dewet the PMMA-rich phase layer and form PS drops suspended in the PMMA matrix. The results show that the surface morphology was controlled by interplay between phase separation and dewetting.

## Acknowledgements

This work is subsidized by the National Natural Science Foundation of China for General (20074037, 50027001, 20274050) and Major (50290090) Program and National Science Fund for Distinguished Young Scholars of China (59825113, 50125311), and the Ministry of Science and Technology of China for Special Pro-funds for Major State Basic Research Projects (2002CCAD4000) and the Special Funds for Major State Basic Research Projects (G1999064800). The authors also thank for the Chinese Academy of Sciences for Distinguished Talents Program and Intellectual Innovations Project (KGCX2-205-03), and Jilin Province for Distinguished Young Scholars Fund (20010101).

## References

[1] Walheim S, Böltau M, Steiner U, Krausch G. Phase separation in thin films of strongly incompatible polymer blends. In: Richards RW, Peace SK, editors. Polymer surfaces and Interfaces III. Chichester: Wiley; 1999. p. 75–99.

[2] Walheim S, Schäffer E, Mlynek J, Steiner U. Science 1999;283:520.
[3] Böltau M, Walheim S, Mlynek J, Krausch G, Steiner U. Nature 1998; 391:877.
[4] Venugopal G, Krause S. Macromolecules 1992;25:4626.
[5] Kokkinos IG, Kosmos MK. Macromolecules 1997;30:577.
[6] Hariharan A, Kumar SK, Russell TP. Macromolecules 1991;24:4090.
[7] Hariharan A, Kumar SK, Russell TP. Macromolecules 1990;23:3584.
[8] Sokolov J, Rafailovich MH, Jones RAL, Kramer EJ. Appl Phys Lett 1989;54:590.
[9] Jones RAL, Norton LJ, Kramer EJ, Composto RJ, Stein RS, Russell TP, Mansour A, Karim A, Felcher GP, Rafailovich MH, Sokolov J, Zhao X, Schwarz SA. Europhys Lett 1990;12:41.
[10] Zhao X, Zhao W, Sokolov J, Rafailovich MH, Schwarz SA, Wilkens BJ, Jones RAL, Kramer EJ. Macromolecules 1991;24:5991.
[11] Hong PP, Boerio F. Macromolecules 1994;27:596.
[12] Bhatia QS, Pan DH, Koberstein JT. Macromolecules 1988;21:2166.
[13] Tanaka K, Takahara A, Kajiyama T. Macromolecules 1996;29:3232.
[14] Ton-That C, Shard AG, Teare DOH, Bradley RH. Polymer 2000;42: 1121.
[15] Walheim S, Böltau M, Mlynek J, Krausch G, Steiner U. Macromolecules 1997;30:4995.
[16] Geoghegan M, Jones RAL, Clough AS, Penfold J. J Polym Sci Part B: Polym Phys 1995;33:1307.
[17] Tanaka K, Takahara A, Kajiyama T. Macromolecules 1998;31:863.
[18] Wool RP. Polymer interface. Munchen: Carl HanserVerlag; 1995.
[19] Müller-Buschbaum P, Gutmann JS, Stamm M. Macromolecules 2000; 33:4886.
[20] Müller-Buschbaum P, O'Neill SA, Affrossman S, Stamm M. Macromolecules 1998;31:5003.
[21] Winesett DA, Ade H, Sokolov J, Rafailovich MH, Zhu S. Polym Int 2000;49:458.
[22] Winesett DA, Zhu S, Sokolov J, Rafailovich M, Ade H. High Perform Polym 2000;12:599.
[23] Ton-That C, Shard AG, Daley R, Bradley RH. Macromolecules 2000; 33:8453.
[24] Harris M, Appel G, Ade H. Macromolecules 2003;36:3307.
[25] Ellingson PC, Strand DA, Cohen A, Sammler RL, Carriere CJ. Macromolecules 1994;27:1643.
[26] Claveland JP, Anczykowski B, Schmid AE, Elings VB. Appl Phys Lett 1998;72:2613.
[27] Bar G, Thomann Y, Brandsch R, Cantow HJ, Wangbo MH. Langmuir 1997;13:3807.
[28] Magonov SN, Ellings V, Whangbo MH. Surf Sci 1997;375:L385.
[29] Tamayo J, Garcia R. Langmuir 1996;12:4430.
[30] Vishwanathan R, Tian J, Marr DWM. Langmuir 1997;13:1840.
[31] Bar G, Thomann Y, Wangbo MH. Langmuir 1998;14:1219.
[32] Luzinov I, Julthongpiput D, Tsukruk VV. Macromolecules 2000;33: 7629.
[33] Tanaka H. J Phys Condens Matter 2000;12:R207.
[34] Qu S, Clarke J, Liu Y, Rafailovich MH, Sokolov J, Phelan KC, Krausch G. Macromolecules 1997;30:3640.
[35] Lau WWY, Burns CM, Huang RYM. J Appl Polym Sci 1994;29:1531.
[36] Sferrazza M, Xiao C, Bucknall DG, Jones RAL. J Phys Condens Matter 2001;13:10269.
[37] Ton-That C, Campbell PA, Bradley RH. Langmuir 2000;16:5054.
[38] Broseta D, Fredrickson GH, Helfand E, Leibler L. Macromolecules 1990;23:132.
[39] Kressler J, Higashida N, Shimomai K, Inoue T, Ougizawa T. Macromolecules 1994;27:2448.
[40] Higashida N, Kressler J, Yukioka S, Inoue T. Macromolecules 1992; 25:5259.
[41] LeGrand DG, Gaines Jr GL. J Colloid Interf Sci 1969;31:162.
[42] Lambooy P, Phelan KC, Haugg O, Krausch G. Phys Rev Lett 1996;76: 1110.
[43] Wang C, Krausch G, Geoghegan M. Langmuir 2001;17:6269.
[44] Fox TG, Flory PJ. J Polym Sci 1954;14:315.
[45] Fuchs K, Friedrich C, Weese J. Macromolecules 1996;29:5893.